Study of interwell carrier transport by terahertz four-wave mixing in an optical amplifier with tensile and compressively strained quantum wells

Jianhui Zhou, Namkyoo Park, and Kerry J. Vahala
Department of Applied Physics, Mail Stop 128-95, California Institute of Technology, Pasadena, California 91125

Michael A. Newkirk and Barry I. Miller
AT&T Bell Laboratories, Holmdel, New Jersey 07733

(Received 14 February 1994; accepted for publication 11 August 1994)

Interwell carrier transport in a semiconductor optical amplifier having a structure of alternating tensile and compressively strained quantum wells was studied by four-wave mixing at detuning frequencies up to 1 THz. A calculation of transbarrier transport efficiency is also presented to qualitatively explain the measured signal spectra. © *1994 American Institute of Physics.*

Interwell carrier transport in semiconductor quantum well (QW) lasers has been shown to affect both the static and dynamic performance characteristics of these devices, including their maximum modulation bandwidth.[1–7] Since Rideout *et al.*[1] first proposed a well-barrier hole burning model, a number of theoretical analyses[2–7] and experimental investigations, including modulation response measurements,[5,6] picosecond pump-probe,[8,9] and intermodulation distortion measurements[10] have studied these processes.

Four-wave mixing (FWM) in semiconductor traveling-wave amplifiers (TWAs) has recently emerged as an important technique for study of carrier dynamics in semiconductor active layers.[10–13] In this paper, we report on the first investigation of interwell transport in an MQW TWA using a novel FWM technique that enables selective excitation and probing of adjacent quantum wells.

The semiconductor optical amplifier used in these measurements was an InGaAs/InGaAsP MQW TWA operating at 1.5 μm.[14] The active layer contains six alternating-strain (tensile and compressive) InGaAs QWs. The tensile QWs provide predominantly TM gain, while the compressive QWs provide TE gain but have vanishing TM gain. This device therefore enables selective excitation and probing of wells according to strain. We performed FWM experiments on the device using, first, a probe wave having a polarization orthogonal to the pump waves (cross-polarization FWM), and then having the same polarization as the pump waves (copolarization FWM). The experimental arrangement for this study was similar to what we have described in Ref. 13 except here the input beams were combined using a beam splitter to allow independent polarization control. The FWM signal was measured using a high sensitivity optical heterodyne detection system. Three, single-frequency, tunable, Er-doped fiber ring lasers[15] were used as pump, probe, and local oscillators in the measurements.

In a typical measurement, as illustrated in Fig. 1, input beam 1, having optical frequency f_1 and a given polarization (either TE or TM), and input beam 2, having optical frequency f_2 and a polarization at an angle of 45° with respect to beam 1, were coupled into the TWA. For the configuration shown in Fig. 1, TM-polarized beam 1 and the TM component of beam 2 serve as pumps to excite carriers in the tensile wells through interband transitions. Carrier dynamics in the compressive QWs were then probed using the TE-polarized component of beam 2 (cross-polarization FWM), while carrier dynamics in the tensile QWs were probed using the TM-polarized component of beam 2 (copolarization FWM). The cross-polarized (TE) and copolarized (TM) FWM signals at optical frequency $2f_2-f_1$ were measured using the heterodyne detection system in which the TWA output, after passing a polarizer (selecting TE or TM polarization), was mixed with a tunable fiber laser local oscillator. Figure 2 shows the measured cross-polarized (TM pump, TE probe) and copolarized (TM pump and probe) FWM signal powers, normalized by the pump and probe amplitudes, plotted versus the detuning frequency f_2-f_1 (both positive and negative). We also carried out co- and cross-polarization FWM measurements where pump waves were TE polarized. The FWM signal spectra measured for this case are shown in Fig. 3.

As shown in previous conventional FWM studies,[12,13] contributing mechanisms to FWM are interband carrier number modulation and intraband occupancy modulation. The former is characterized by the interband carrier lifetime which is on the order of several hundred picoseconds in QW amplifier devices. The latter typically includes spectral hole burning and dynamic carrier heating. Spectral hole burning results from the finite intraband carrier-carrier scattering time ($<$100 fs), which sets the time scale on which non-Fermi carrier distributions are restored to equilibrium. Carrier heating results from stimulated emission, which removes ''cold''

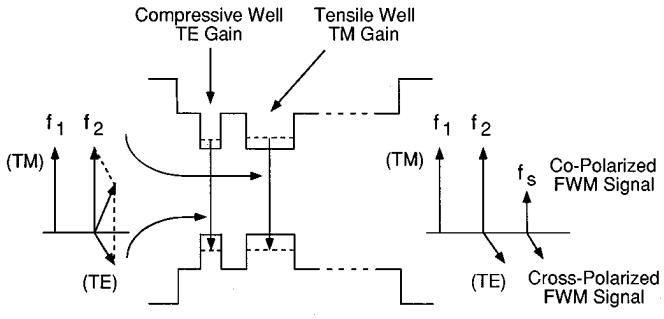

FIG. 1. Diagram of FWM processes in TWA having a structure of alternating tensile and compressively strained quantum wells.

 0003-6951/94/65(15)/1897/3/$6.00

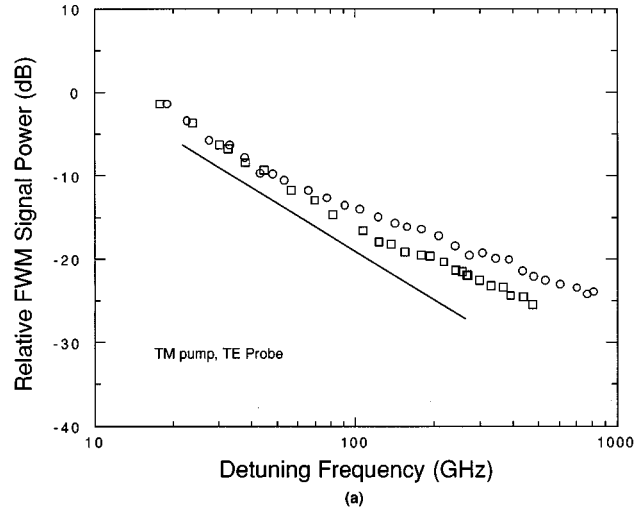

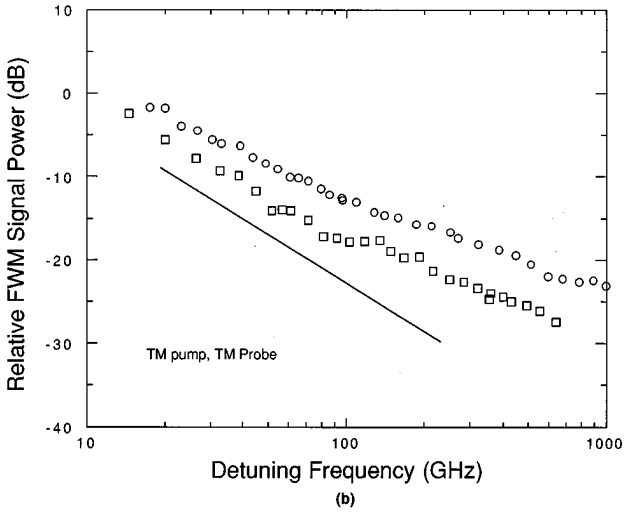

FIG. 2. Relative (a) cross-polarized (b) copolarized FWM signal power measured with TM-polarized pump vs positive (circle), and negative detuning (square) frequencies, showing 20 dB/decade line (solid line).

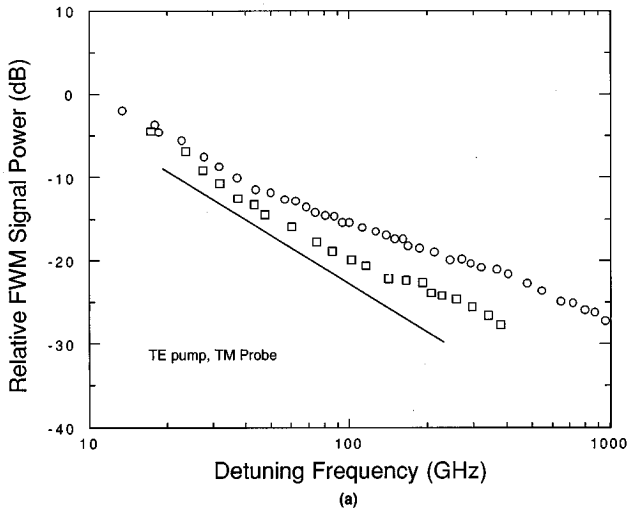

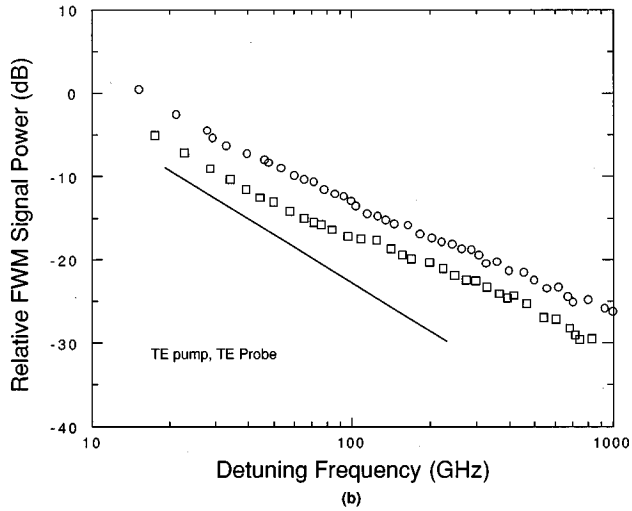

FIG. 3. Relative (a) cross-polarized (b) copolarized FWM signal power measured with TE-polarized pump vs positive (circle), and negative (square) detuning frequencies, showing 20 dB/decade line (solid line).

carriers close to the band edges, and from free-carrier absorption, which transfers carriers to higher energies within the bands. The resulting hot carrier distributions relax to the lattice temperature by emission of optical phonons with a characteristic time constant of about 0.65−1 ps. For the detuning frequencies considered in this measurement, FWM is dominated by carrier number modulation and carrier temperature modulation.

The copolarization signal spectra, as shown in Figs. 2(b) and 3(b), exhibit an asymmetry with respect to positive and negative detuning. This asymmetry has been shown to result from signal phase interferences which occur between the contributing FWM mechanics[12,13] and can be used to determine the relative strengths of the contributing mechanisms.

In order to understand the cross-polarized data, we must also consider interwell transport. Within an excited well, modulation is produced by the same mechanisms described above. These modulations are then coupled into adjacent nonexcited wells through interwell carrier transport processes, generating the cross-polarized FWM signal. The observed difference between the cross- and copolarized spectra should bear the signature of interwell carrier transport. A comparison of these spectra therefore provides a frequency-domain tool for analysis of the interwell transport processes.

For the detuning frequencies of this measurement, interwell transport includes primarily carrier number transport and carrier temperature transport. The interwell carrier number transport can be approximately described as a three-step process. First, 2D carriers in the excited well are coupled to the 3D states in the same well through quantum capture/escape processes. These 3D carriers are then transported to the nonexcited wells through the combined effect of diffusion and drift. Finally, also through carrier capture/escape processes, the transported 3D carriers fall into the 2D states in the nonexcited well, where they contribute to the cross-polarized FWM. For carrier temperature modulation, in addition to the above-mentioned processes, carrier-carrier scattering can also assist the temperature transport.

During the interwell transport process, the two modulations (carrier number and temperature) experience difference

damping mechanisms (i.e., transport of carrier number modulation is damped by spontaneous interband carrier recombination, while the carrier temperature modulation is damped by carrier-lattice interactions having a much shorter relaxation time. These widely different damping rates affect the corresponding interwell transport efficiencies because of their strong dependence on damping.

To illustrate, we calculate the transbarrier transport efficiency by considering 3D carrier transport from an excited well to the adjacent nonexcited well using a simple 1D diffusion equation. The trans-barrier transport efficiency η at detuning frequency Ω is then given by

$$\eta = \exp\left(-\frac{s}{\sqrt{D}} \sqrt{\frac{1}{\tau} - i\Omega} \right),$$

where s is the separation between wells; D and τ are the diffusion constant and lifetime associated with the respective modulations. Since the carrier number damping time ($\sim$200 ps) is much longer than the temperature damping time ($\sim$650 fs), carrier temperature modulation transport is much less efficient than carrier number transport. We have assumed comparable diffusion constants for the two modulations in the above discussion. Another contributing mechanism to the transbarrier transport is drift of 3D carriers caused by internal fields. The drift process, like the diffusion process, also favors the mechanism having the longer time constant so that, assuming all other factors are comparable, carrier number transport is again expected to be more efficient than the carrier temperature transport.

Similarly, the efficiency associated the escape/capture dynamics are also subject to the damping effect. Widely different relaxation time constants for the two modulations should lead to very different efficiencies in the escape/capture process. We would therefore expect overall interwell transport to exhibit a higher efficiency for the carrier number modulation than for the temperature modulation.

As shown in Figs. 2 and 3, the cross- and copolarized FWM signals were found to have comparable amplitudes at low frequencies. Furthermore, the cross-polarized FWM data in Figs. 2(a) and 3(a) do not show any roll-off induced by the carrier number transport (i.e., beyond the 20 dB/decade roll-off caused by the interband modulation within the excited wells). This indicates that carrier number modulation, which is responsible for the low frequency data, is coupled from excited wells to nonexcited wells with little loss. This agrees qualitatively with a calculation of the trans-barrier transport efficiency function which gives $|\eta| > 78\%$ for $\tau = 200$ ps, $D = 5\ \mathrm{cm}^2\,\mathrm{s}^{-1}$, $s = 100$ Å, and $\Omega/2\pi < 100$ GHz. It also suggests that the interwell carrier-number transport in the present device is fast enough so that carrier number modulation in nonexcited wells behaves as if it were generated within these wells for frequencies at least as high as 100 GHz (beyond this frequency the modulation data is obscured by the presence of additional mechanisms, making prediction of a definitive upper transport rate impossible).

The cross-polarized FWM signal spectra are symmetrical at low frequencies with respect to positive and negative detuning in contrast to the copolarized FWM spectra, which show a steady asymmetry. As shown in the above calculation and discussion, transport of carrier number modulation is much more efficient than the transport of temperature modulation, especially at frequencies lower than the corner frequency of the carrier heating effect ($\sim$250 GHz). [As indicated in the expression for η, the transbarrier transport efficiencies become comparable beyond this frequency.] Phase interferences are therefore suppressed in the cross-polarized measurement at low frequencies, causing the highly symmetrical spectra.

Finally, it should be mentioned that carrier heating induced by free-carrier absorption is not strain selective. Specifically, it can take place in both types of wells when pumps are TE polarized, but it is inhibited in all wells when pumps are TM polarized due to the QW confinement barrier. Therefore, temperature modulation within the nonexcited wells is potentially significant in the case of TE pumps. This might explain the observed difference in the two sets of cross-polarized spectra at low detuning frequencies, where data with TE pumps show an earlier onset of reduced symmetry (i.e., more phase interference between carrier number and temperature modulations).

In summary, we have measured co- and cross-polarization FWM up to 1 THz in a TWA having alternating tensile and compressively strained QWs. The effect of interwell carrier transport on FWM signal spectra is observed and a possible explanation is provided by noting the different transbarrier transport efficiencies for carrier number and temperature modulations. It is important, however, to point out that the complexities of this system require a more sophisticated theoretical treatment.

This work was supported by the Office of Naval Research (Contract N00014-91-1524) and Northrop Corporation.

[1] W. Rideout, W. F. Sharfin, E. S. Koteles, M. O. Vassell, and B. Elman, IEEE Photo. Tech. Lett. **3**, 784 (1991).
[2] R. Nagarajan, T. Fukushima, S. W. Corzine, and J. E. Bowers, Appl. Phys. Lett. **59**, 1835 (1991).
[3] S. C. Kan, D. Vassilovski, T. C. Wu, and K. Y. Lau, Appl. Phys. Lett. **61**, 752 (1992).
[4] S. C. Kan, D. Vassilovski, T. C. Wu, and K. Y. Lau, Appl. Phys. Lett. **63**, 2307 (1993).
[5] R. Nagarajan, M. Ishikawa, T. Fukushima, R. S. Geels, and J. E. Bowers, IEEE J. Quantum Electron. **28**, 1990 (1992).
[6] M. Ishikawa, R. Nagarajan, T. Fukushima, J. G. Wasserbauer, and J. E. Bowers, IEEE J. Quantum Electron. **28**, 2230 (1992).
[7] N. Tessler and E. Eisenstein, IEEE J. Quantum Electron. **29**, 2230 (1993).
[8] G. Eisenstein, J. M. Wiesenfeld, M. Wegener, G. Sucha, D. S. Chemla, S. Weiss, G. Raybon, and U. Koren, Appl. Phys. Lett. **58**, 158 (1991).
[9] S. Weiss, J. M. Wiesenfeld, D. S. Chemla, G. Raybon, G. Sucha, M. Wegener, G. Wisenstein, C. A. Burrus, A. G. Dentai, U. Koren, B. I. Miller, H. Temkin, R. A. Logan, and T. Tanbun-Ek, Appl. Phys. Lett. **60**, 9 (1992).
[10] Y. C. Chung, J. M. Wisenfeld, G. Raybon, U. Koren, and Y. Twu, IEEE Photon. Tech. Lett. **3**, 130 (1991).
[11] L. F. Tiemeijer, Appl. Phys. Lett. **59**, 499 (1991).
[12] K. Kikuchi, M. Kakui, C. E. Zah, and T. P. Lee, IEEE J. Quantum Electron. **28**, 151 (1992).
[13] J. Zhou, N. Park, J. W. Dawson, K. J. Vahala, M. A. Newkirk, and B. I. Miller, Appl. Phys. Lett. **63**, 1179 (1993)
[14] M. A. Newkirk, B. I. Miller, U. Koren, M. G. Young, M. Chen, R. M. Jopson, and C. A. Burrus, IEEE Photon. Tech. Lett. **5**, 406 (1993).
[15] N. Park, J. W. Dawson, K. J. Vahala, and C. Miller, Appl. Phys. Lett. **59**, 2369 (1991).